NEAR-SHORE OCEANIC EARTHQUAKES: APPLICATION OF ACOUSTIC METHODS TO DETECT EARTHQUAKE PRECURSORY PHENOMENA AND POSSIBLE IMPROVEMENTS OF TSUNAMI WARNING SYSTEMS*

Elena V. Sassorova[1]; Igor N. Didenkulov[2]; Yakov S. Karlik[3]; Boris W. Levin[1]; Victor E. Morozov[1]; Sergey P. Petrochenko[4]

[1] P. P. Shirshov Institute of Oceanology RAS, Moscow, Russia
[2] Institute of Applied Physics RAS, Nizhny Novgorod, Russia
[3] Institute "Morphyspribor", Sankt-Peterburg, Russia
[4] V. I. Ilychev Pacific Oceanological Institute FEB RAS, Vladivostok, Russia
E-mail: **sasor@sio.rssi.ru, levin@rfbr.ru**

1. INTRODUCTION

The problem of local tsunami warning remains almost unsolved up to now both theoretically and practically for near-shore seismic events. So called "local tsunamis" are formed within approximately 50 – 100 km offshore, so their propagation time from the source to the coast is less than 1 hour. Shortage of time makes these tsunamis particularly dangerous.

Figure 1 shows locations of tsunamigenic earthquake epicenters (earthquakes with magnitudes $M_S > 6.0$) near the Kamchatka Peninsula over a period of 50 years (from 1950 to 2000). Data were extracted from the Expert Tsunami Data Base for the Pacific Ocean (ETDB) collected, created and supported by the Tsunami Laboratory (Novosibirsk Institute ICMG SB RAS). Most of the earthquake epicenters, which are marked by solid circles with different diameters (depending on the earthquake magnitude), are located in the near-shore zone (less than 70 km offshore). Solid black line in Figure 1 is the oceanic tectonic plate boundary.

The information on these earthquakes (dates, coordinates, depth, magnitude, maximum runup) is presented in Table 1. The right column shows minimum distance to the coastline (letters C/L for earthquakes that occurred just under the coastline). Mean offshore distance for all listed events is a little less than 18 km. The bottom part of the table contains rough estimates of tsunami propagation speed and tsunami travel time for the mean distance. It follows from these estimates that tsunami waves arrive at the coast within 7.5 min after the seismic event. It is obviously impossible to declare timely tsunami warnings based either on tide-gauges or seismic information. The situation is the same for the Pacific coast of the Kuril Islands.

A possible way to solve this problem is detection and recording of signals preceding major underwater near-shore earthquakes, i.e. certain signs of the earthquake preparation or of the critical state of the near-focal zone.

This work is based on hydroacoustic systems for studying both the variations of low-frequency noise appearing during the earthquake preparation, and hydroacoustic signals from microseismic sources inside the near-focal zone.

* Translated by O. I. Yakovenko, edited by A. B. Rabinovich and D. Weichert

Table 1

Tsunamigenic earthquakes near Kamchatka Pacific coastline (1950-2000, M>5.0).

Date	Lat	Lon	Depth km	Ms	Hmax m.	Dist. km.
04.11.52	52.75	159.5	30	8.2	20	43
17.03.53	50.00	156.4	70	6.2	3	43
04.05.59	53.40	159.6	30	7.7	2	C/L
10.01.61	50.02	156.2	68	7.1		32
22.11.69	57.73	163.6	8	7.3	15	17
15.12.71	56.02	163.2	26	7.8	0.47	5
28.02.73	50.48	156.6	60	7.5	1.5	20
17.08.83	55.79	161.3	93	6.7	0.02	C/L
28.12.84	56.21	163.4	19	7.0	0.02	1
08.06.93	51.20	157.8	60	7.2	0.5	29
13.11.93	51.94	158.6	35	7.0	0.1	25
05.12.97	54.83	162.0	34	7.7	1.5	C/L

the mean distance	17,92 km.
the mean ocean depth	160 m
the mean velocity	40 m/s
the mean travel time	7,5 min

$\mathbf{H_{max}}$ maximum wave height
L – shortest distance from the epicenter to the shoreline.

2. ACOUSTIC EMISSION DURING THE EARTHQUAKE PREPARATION

The appearance of acoustic signals in the frequency range of 0.01-1 kHz just before the earthquake was discussed by several authors. Rykunov [1978, 1979, 1992] was probably the first to study seismic emission of a medium in the frequency range 30-40 Hz. Concentration of tangential stress preceding major earthquakes causes modification of the medium properties in focal and adjacent zones. Michihiro *et al*. [1989], Sobolev [1993], and Saltykov *et al*. [1998] found increase of seismic emission activity near foci during the period of earthquake preparation and decrease immediately after the event (i.e. after the state-strain discharge into the medium). Belyakov and Nikolaev [1991, 1995] studied acoustic signals from seismometer wells in the frequency range 10 Hz – 1 kHz; their efforts were directed towards examination of the properties of the geophysical environment and their link to the stressed state of the medium. Recently, Kamchatka scientists [Saltykov, 1995; Saltykov *et al.*, 1997, 1998] made a thorough study of the seismic emission during the process of earthquake preparation. Seismo-acoustic signals strongly depend on anthropogenic factors and decay quickly with distance. Above-mentioned phenomena had been observed at surface stations, and the studied acoustic signals reflected mainly modifications of the properties of big blocks in the stressed medium.

Laboratory experimental studies by Sassorova *et al*. [2001] and Mostriukov *et al*. [2002] were dedicated specifically to examination of signals, which appear before sample destruction ("stick-slip" model). We found 4 types of signals. Three of them are shown in Figure 2. Two of these four types (A and B) are high-frequency acoustic signals. In the first case (A), a short high-frequency pulse packet arises, but is soon damped out.. In the second case (B), an acoustic signal, which arises just before the destruction, lasts to the beginning of the destruction itself. In the third case (C), a low-

frequency signal arises before the destruction and lasts up to the very event. Scheme of the experimental model is shown in Figure 3. We interpreted the signals of the first type as the micro-destruction on the contact surface before the blocks slip. Only the sensors closest to the micro-destruction site clearly recorded the signals. In particular, all sensors reliably recorded the third type of signals (low-frequency). Micro-destruction signals have smaller amplitude, significantly higher frequency and decay very fast.

Laboratory experimental studies by Sassorova *et al*. [2001] and Mostriukov *et al*. [2002] were dedicated specifically to examination of signals, which appear before sample destruction ("stick-slip" model). We found 4 types of signals. Three of them are shown in Figure 2. Two of these four types (A and B) are high-frequency acoustic signals. In the first case (A), a short high-frequency pulse packet arises, but is soon damped out.. In the second case (B), an acoustic signal, which arises just before the destruction, lasts to the beginning of the destruction itself. In the third case (C), a low-frequency signal arises before the destruction and lasts up to the very event. Scheme of the experimental model is shown in Figure 3. We interpreted the signals of the first type as the micro-destruction on the contact surface before the blocks slip. Only the sensors closest to the micro-destruction site clearly recorded the signals. In particular, all sensors reliably recorded the third type of signals (low-frequency). Micro-destruction signals have smaller amplitude, significantly higher frequency and decay very fast.

Smirnov *et al.* [1995 a, 1995 b, 2001] and Ponomarev *et al.* [1997]] examined formation and evolution of acoustic signals in the experiments on sample destruction. Loading regime with negative feedback in acoustic activity was used during these experiments. The acoustic emission intensity increased and the rate of loading decreased. That allowed extending the time of the initial stage of micro-rupture formation. Figure 4, taken from [*Smirnov et al*., 1995], shows the process of micro-destruction formation and the location of these destructions along the body of the sample as function of the loading growth. This process causes significant increase of the acoustic emission intensity. Initially, the micro-destructions are located chaotically; then they begin to concentrate in the zone of the future macro-destruction. So, the experimental works confirm the origin of high-frequency acoustic signals during the stage of the destruction preparation process.

Figure 1. Tsunamis caused by earthquakes near the Kamchatka Pacific coastline (years 1950-2000, $M > 5.0$). Thick solid line is the ocean trench line; solid circles are the epicenters of the earthquakes.

Figure 2. Acoustic signal preceding the main rupture process in laboratory experiments ("stick-slip" model).

Figure 3. Scheme of the laboratory experiment ("stick-slip" model). The circles with numbers are ultrasonic sensors.

Figure 4. The results of laboratory experiments made by Smirnov *et al*. [1995].

Figure 5. The Regional Catalog and timetable of the digital records on the time axis: Fragments for 20 (a), 24 (b), and 28 (c) October 1998.

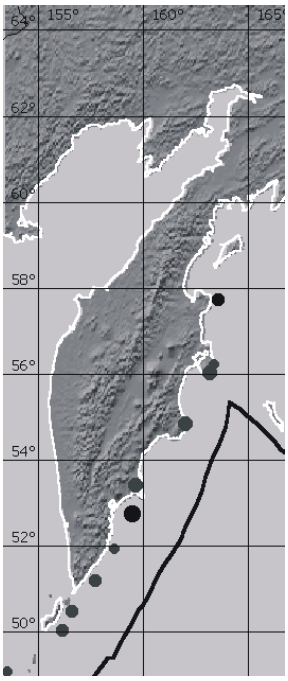

Figure 1.

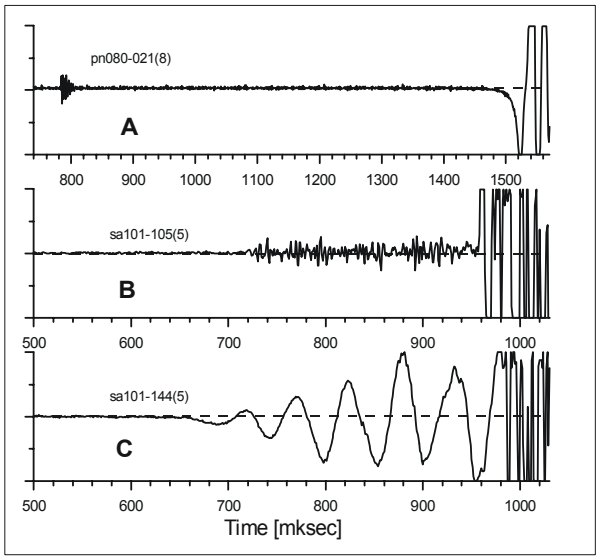

Figure 2.

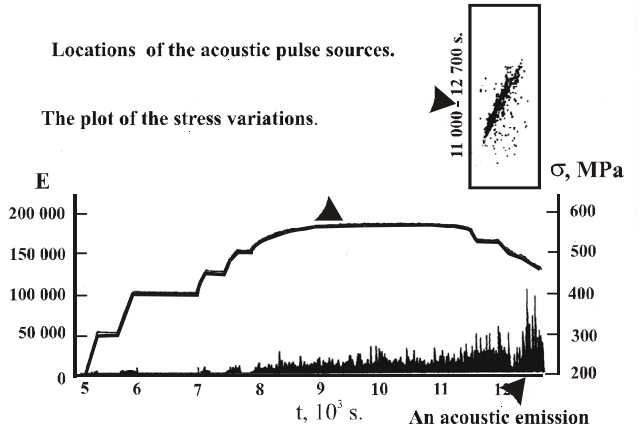

Figure 4.

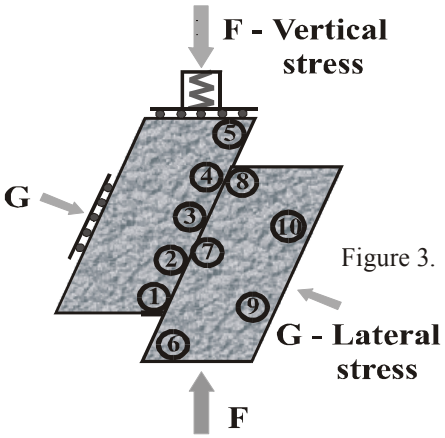

Figure 3.

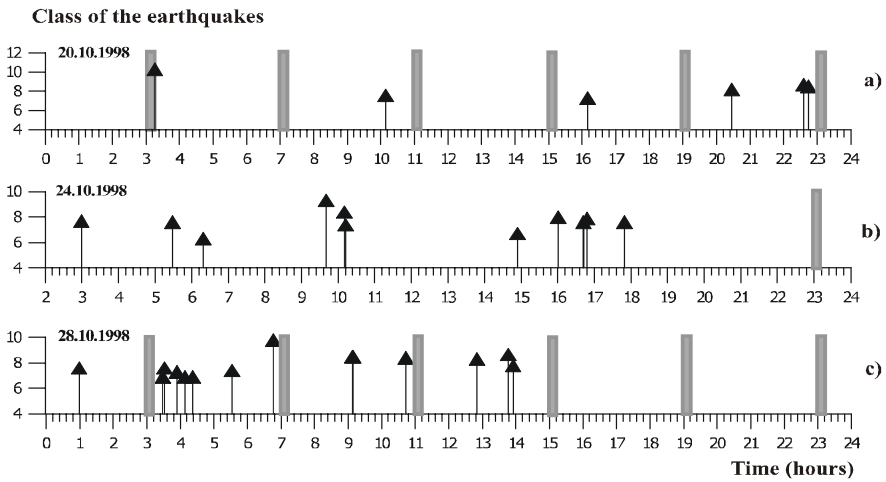

Figure 5.

These experimental results give an important theoretical basis to extract and analyze high-frequency acoustic signals, which have been emitted from the near-focal zone of the future rupture. These signals are apparently related to formation of small fissures and micro-ruptures during the earthquake preparation process. So, several suggestions are made on possible application of seismo-acoustic signals as one of the key signs of the earthquake preparation.

DAMPING OF THE ACOUSTIC SIGNALS IN SOLID MEDIA AND WATER

Soloviev *et al*. [1989a,b] used a combined net of inland (surface) and sea-bottom seismic stations to study the seismicity of the Aegean and Tyrrhenian seas. They found that bottom observations give significantly larger number of recorded earthquakes. During continuous 8-day observation period in the Aegean Sea, the bottom stations recorded 420 earthquakes, and the hypocenters were identified for 134 events with magnitude $M_L \le 4$. In contrast, only 2 events with magnitude $M_L = 4$ were fixed during the same time by the inland stations in Central Greece. Three regional near-shore stations recorded 10, 10, and 32 events. The situation was similar during 10-day experiments in the Tyrrhenian Sea. So, it is obvious, that seismic signals from weak earthquakes decay completely in sedimentary layers, and are practically not recorded by surface stations.

Decay (absorption) of the plane sound wave in the medium follows the law: $I(x) = I_0 \cdot \exp(-\beta x)$, where β is the coefficient of the energetic absorption, I_0 is the wave energy in the source, and $I(x)$ is wave energy at the distance x from the source; damping factor is measured in m^{-1} or in km^{-1}. This expression may be re-written in decibels with ordinary damping factor. Then we obtain: $a_{dB} = 4.34\beta$, where a_{dB} is expressed in dB/m or in dB/km.

Sound decay in water occurs at frequencies approximately up to 1000 Hz and is proportional to the frequency square, i.e. $\beta \sim f^2$. For frequency of 100 Hz the damping factor is about a_{dB} (100 Hz) = 0.0006 dB/km, and respectively β (100 Hz) = 0.00014 km^{-1}. Therefore, at frequency 100 Hz sound absorption is negligible, and we do not need to consider it for distances less than 1000 km [Clay and Medwin, 1977].

The sound decay in solid rocks is several orders faster than in water. The sound absorption in sediments and in hard rocks is proportional to the sound frequency. Both for rocks and sedimentary rocks, the law of linear dependence of the damping factor on frequency is valid: $a_{dB}(\mathrm{dB/km}) = b \cdot f(\mathrm{Hz})$; the frequency f is measured here in Hz, b is measured in dB/(km·Hz), and a_{dB} in dB/km [Clay and Medwin, 1977; Sheriff and Geldart, 1995].

1) Solid (magmatic) rocks 0.01;
2) Clay, silt (sediments) 0.1;
3) Sand 0.5.

Thus, wave decay at frequency 10 Hz in solid rocks is about 0.1 dB/km, in sedimentary rocks 1 dB/km, and in sand 5 dB/km. At frequency 100 Hz these values will be approximately 10 times higher. It should be noted that the numbers above are typical mean values. For every specific case the real values may different.

Based on the relations given above, the signal in solid rocks will almost vanish at the distance of 50 km for frequencies of 50 Hz (and higher) ($I(x)/I_0 < 3.0 \cdot 10^{-3}$); in sedimentary rocks this will occur at the distance of 10 km for frequencies of 30 Hz and higher ($I(x)/I_0 < 9.0 \cdot 10^{-4}$), and in sand this will take place at the distance of 2 km for frequencies of 30 Hz and higher.

Increase of mechanical stress in the Earth's crust, formation of fissures and partial destruction of solid rocks precede a seismic event [Vinogradov, 1989], stimulating emission of the acoustic waves. Periods of these waves depend on size of the destruction zones, which are relatively small in comparison with those formed during the earthquake itself. This is the reason why, they first emit high-frequency waves.

Levin and Sassorova [1999, 2001] presented the relationship obtained after the analysis of observational and physical model data. This relationship relates the size of the area emitting a seismic signal formed during the destruction preparation, to the period of the generated signal. Table 2 presents evaluation of the destruction-area dimension as a function of the frequency of the emitted signal. So, acoustic signals in the range of 1 kHz are normally emitted by sources smaller than 10 cm, and the size of the source generating signals with frequencies of 10-30 Hz should be significantly larger (between 1000 and 100 meters, respectively.

Table 2

Evaluation of the destruction-area dimension as a function of the frequency of the emitted signal.

Frequency, Hz	10	20	30	40	50	60	75	100	1000	1500
Size of the oscillation zone, m	986	246	109	62	40	27	18	10	0.1	0.04

In accordance with these simple estimates, acoustic signals generated by small destruction sources will decay rapidly in solid media. This is the reason why surface stations rarely record these signals coming from the near-focal zone.

Decay of the acoustic signal in water (layer of incompressible fluid) is one half of that in solid medium, and four times smaller than in sediment layers. Due to this fact, we can suggest that hydroacoustic systems, installed in the ocean, could record precursory acoustic signals of strong earthquakes, which cannot be recorded onshore. In general, the idea to record the acoustic signals in the ocean and to use these signals as predictors of strong oceanic earthquakes looks very promising.

SHORT DESCRIPTION OF HYDROACOUSTIC DATA

Hydroacoustic study experience shows that among the large amount of information on oceanic noises, caused by moving and motionless human-made objects, it is possible to extract information related to the preparation and occurrence of oceanic earthquakes. High correlation of hydroacoustic signals with seismic signals had been noticed long time ago, however almost nobody has tried to use this information to examine earthquake process preparation.

Recently, we had the opportunity to analyze the signals recorded by an antenna of the "Agam" type (developed in the Institute "Morphyzpribor", Sankt Petersburg), which is situated near the eastern coast of Kamchatka in the Pacific Ocean [cf. Demianovich,

1998; *Karlik*, 2002]. In particular, we were able to use the data of the 1998-1999 International program "ATOC" (Acoustic Thermometry of the Oceanic Climate). This allowed us for the first time to detect and examine the acoustic signals from oceanic earthquake sources. The antenna was submerged into the water and deployed near the bottom; its size was 100×17 m [Demianovich, 1998; Karlik, 2002]. Several hundred hydrophones were grouped in separated blocks (channels, clusters) that allowed detecting the direction to the source based on time lags in signal arrivals to different channels.

The material obtained during the experiment ATOC contained 162 continuous records covering the period of 12.07.1998 to 21.03.1999. The length of each record was of 1323.73 sec (point in English, comma in French, German and other languages)(a little more than 22 min), every day there were up to 6 scheduled records (performed at 2:54:20, 6:54:20, 10:54:20, 14:54:20, 18:54:20, 22:54:20 GMT). However, on some days there were no records and on some others there were only a few. The sampling rate of the records was 300 Hz, the frequency range from 40 to 110 Hz was isolated by the band-pass instrumental filter. The records were from different seasons, daytime and weather conditions; so we could thoroughly examine the acoustic background. During the experiment there were 14 working channels of the antenna. The total observational period was 276 days, and the summation length of all records was 3564 minutes or 2.475 days. During this observational period 3058 seismic events occurred in the Kamchatka area (48^o-60^o N, 151^o-173^o E) according to the Regional Earthquake Catalog. The main purpose of this study was comparison of seismic and hydroacoustic signals (HAS) and detection of the sources of the seismic signal "emitters".

COMBINED ANALYSIS OF THE HYDROACOUSTIC SIGNALS AND THE REGIONAL EARTHQUAKE CATALOG

We examined only that part of the Regional Earthquake Catalog, which corresponds to the time period of 12.07.1998 to 21.03.1999. Sections of the time axis for October 20, 24 and 28, 1998 are given in Figures 5a, 5b, and 5c, respectively. In the diagram, the horizontal axis is time in hours, and the vertical axis is the earthquake class. Solid vertical lines with arrows at the top mark earthquakes, squares show the time intervals (sessions), when the hydroacoustic records were made.

We found one case of complete time coincidence between the seismic event that started inside the source at 03:15:46 and the HAS record (record of 20.10.1998, 1st session lasted from 02:54:20 till 03:16:24). The beginning of the earthquake was felt at the very end of the session. According to the Regional Catalog, the energy class of the earthquake was K = 10.3, the depth of the hypocenter was 119 km, the horizontal distance from the epicenter to the receiver was 50.4 km, and the distance from the hypocenter was 129.23 km. There were also a few events, when earthquakes occurred soon after the end of the record. For all these cases, we found series of distinct signals emitted form the sources located close to the epicenters, which arrived ahead of the seismic signals.

We identified two types of the signals preceding the main shock. The first type combines micro-earthquake (MEQ) signals arriving from the near-focus zone and emitting acoustic signals in the frequency range 40-75 Hz, which last for 3-4 sec and have very sharp amplitude variations within the first 1-2 seconds (20 times HAS amplitude amplification over the background level). Table 3 gives data for 9 MEQs, detected during the 1st recording session of 20.10.98. The high-amplitude part of the

signal has frequency of 60-75 Hz, then both the amplitude and frequency decrease (frequency decreases up to 40-50 Hz). The second type of detected acoustic signals is high-frequency noise (30-40 Hz) with amplitudes 4 times greater than the background level. The noise appears just before the earthquake (see Table 3) and then merges with the seismic signal from the major shock.

Table 3 gives estimated values of the destruction zone size for every MEQ, calculated from the signal frequency with maximum amplitude. Figure 6a shows a spectrogram of the HAS record made on 20.10.1998 (1st session lasted from 02:54:20 till 03:16:24). Figure 6b is the original digital record for the case when the HAS and the earthquake coincided. In the spectrogram, the intensity of the black color at each point shows the energy of the respective frequency at the given time. There are several sections where the micro-earthquakes, preceding the main shock, are clearly seen. Nine such sections are isolated in Figures 6a and 6b. The high-frequency noise visible at the end of the record (Figure 6b) is shown as a separated section in Figure 7f.

Table 3

MEQ's and the seismic noise time sequence in the hydro-acoustic record (20.10.1998, the first observation session from 02:54:20 up to 03:16:24). MEQ's and the seismic noise parameters.

Time sequence of events	Arrival time (start time) (h:min:sec)	Time before previous event start (min:s)	Estimation tS-tP, s	Source depth estimation for MEQ (under the ocean bottom), m	Signal frequency Hz	Signal source size estimation, m
Beginning of the session	02:54:20	-	-	-	-	-
MEQ №1	03:03:39.51	09:19.51	0.083	191(207)	65	23
MEQ №2	03:05:47.57	02:08.06	0.093	214(232)	59	28
MEQ №3	03:07:35.86	01:48.09	0.103	237(258)	61	26
MEQ №4	03:09:00.42	01:24.56	0.143	329(358)	58	29
MEQ №5	03:10:03.22	01:02.08	0.07	161(175)	73	18
MEQ №6	03:11:55.98	01:52.76	0.08	184(200)	75	17
MEQ №7	03:13:11.45	01:15.47	0.08	184(200)	55	33
MEQ №8	03:14:24.16	01:12.72	0.057	131(143)	62	22
MEQ №9	03:15:45.78	01:21.62	0.087	200(218)	71.5	19
Noise arrival	03:16:05.20	00:19.14	-	-	43	53
end of the session	03:16:23.73	00:18.51	-	-	-	-

Figure 7 shows sections of the same record (for the 1st channel). These sections with equal length (1000 samples or of approximately 3.3 sec) contain micro-earthquakes (7a-e), and high-frequency noise (7f), which appeared just before the main shock.

All these MEQ events have been reliably recorded by all 14 channels of the antenna, the character of the signal from the same MEQ at different channels was almost identical. Only the arrival times to the channels were different that allowed us to identify the direction towards the signal source [Morozov, 2002]. The micro-earthquakes detected from the record of 20.10.1998, and the epicenter of the main shock were located at almost the direction coinciding with the antenna axis.

Only compression (acoustic) waves propagate in water. At the earth/ocean interface, tangential-stress shear waves propagating in solid medium convert into normal-stress waves in water. Difference in the arrival times of these waves to the antenna enables us to estimate the distance between a micro-earthquake focus and the interface (bottom area where these waves emit into the water). Table 3 shows us that the difference in the arrival times between the P-wave and transformed S-waves is about 0.1 sec. Thus, we can conclude that the destructions do not occur in the vicinity of the hypocenter, but in the near-interface zone. This table presents estimated distances between the source of each MEQ and the interface for the event of 20.10.1998. If the earthquake epicenter would be farther from the recording site, the character of the HAS records would change much more. At the solid-liquid interface, a sizeable region emits the acoustic signal; then this signal is summed up during the recording.

In those cases when the earthquake started within few dozens of minutes after the end of the recording, it was possible to detect only micro-earthquakes preceding the major shock. Such records exist for all six sessions of 5.02.1999. Eight earthquakes occurred during this day, but none of them after the time period 06:54:20–07:16:24. Figure 8a shows spectrograms for all sessions of this day. Figure 8c shows an extract from the Regional Earthquake Catalog and the digital records superposed in the time axis. The micro-earthquakes are clearly seen in all spectrograms except the 6 a.m. record; after the completion of this very session no earthquakes occurred for more than four hours. The analysis of other records, preceding earthquakes, gives us similar situations.

A few seismic stations, belonging to the Local System, are located at the southeastern Kamchatka coast where the epicenter region of the 20.10.1998 earthquake was located. We selected 3 stations, which are the nearest to the epicenter: GRL located in the area of Volcano Gorely, RUS located in Bay Russkaya, and PET located in Petropavlovsk-Kamchatsky. These stations (Figure 9) run regular seismic observations and transmit all records via radio channel (with digitization frequency of 128 samples per second at the receiver). The records are stored in archives. We analyzed records from all three stations, which started at 00-00 GMT on 20.10.1998. A certain increase in seismic activity occurred within a few minutes before the earthquake but it was impossible to detect reliable micro-events. The most likely explanation is that the high-frequency seismic signals associated with respective micro-earthquakes decay in solid and sedimentary rocks and become apparent only in liquid layer.

CONCLUSIONS

Combined analysis of digital hydroacoustic records and the Kamchatka Regional Earthquake Catalog enabled us to select HAS (hydroacoustic signal) records coincided with seismic events or preceded them. Two types of signals, preceding earthquakes, have been detected:

- A series of micro-earthquakes, occurring in the near-focal zone, which generated signals in the frequency range of 40-75 Hz and duration of 3-4 sec within more than 1 hour before the major shock. Their sources were different but located nearby.
- High-frequency noise (20-40 Hz) appearing within a few seconds before the earthquake and then merged with the seismic signal from the major shock.

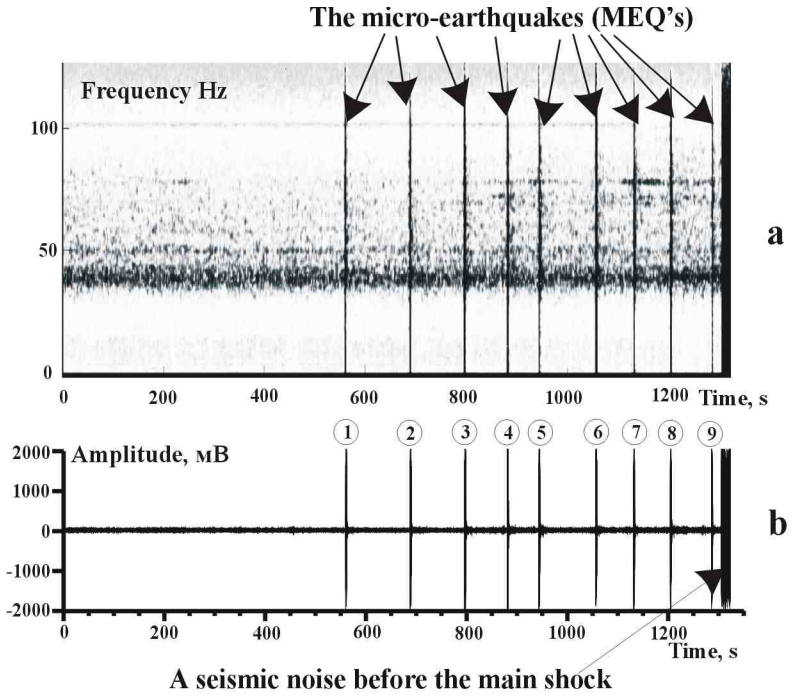

Figure 6. The coincidence of the hydro-acoustic observation session (20.10.1998, from 02:54:20 to 03:16:24) and the earthquake of 20.10.1998 (origin time 03:15:46, Lat. = 52.506 N, Long. = 158.0690 E; Depth = 119 km, $M = 4.6$, $K = 10.3$). (a) spectrogram of the hydroacoustic record, (b) .the record itself.

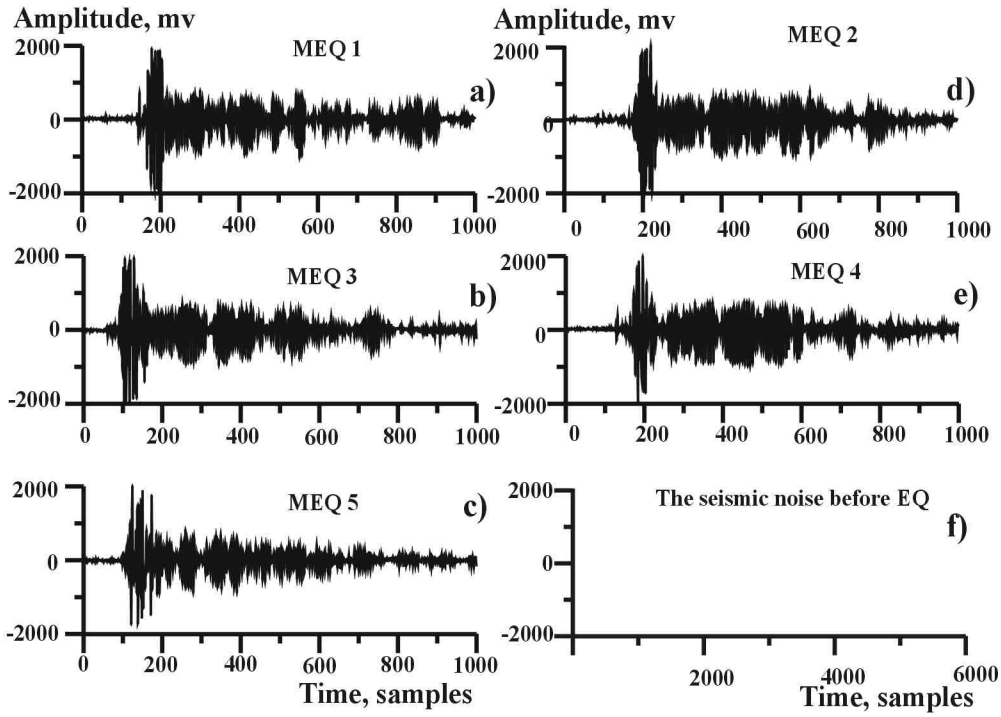

Figure 7. October 20, 1998: Fragments of the hydro-acoustic record (1st channel, observation session from 02:54:20 up to 03:16:24), five MEQ's and seismic noise. Horizontal axis is time (in samples), vertical axis is amplitude (in mV), the section duration is about 3.3 sec.

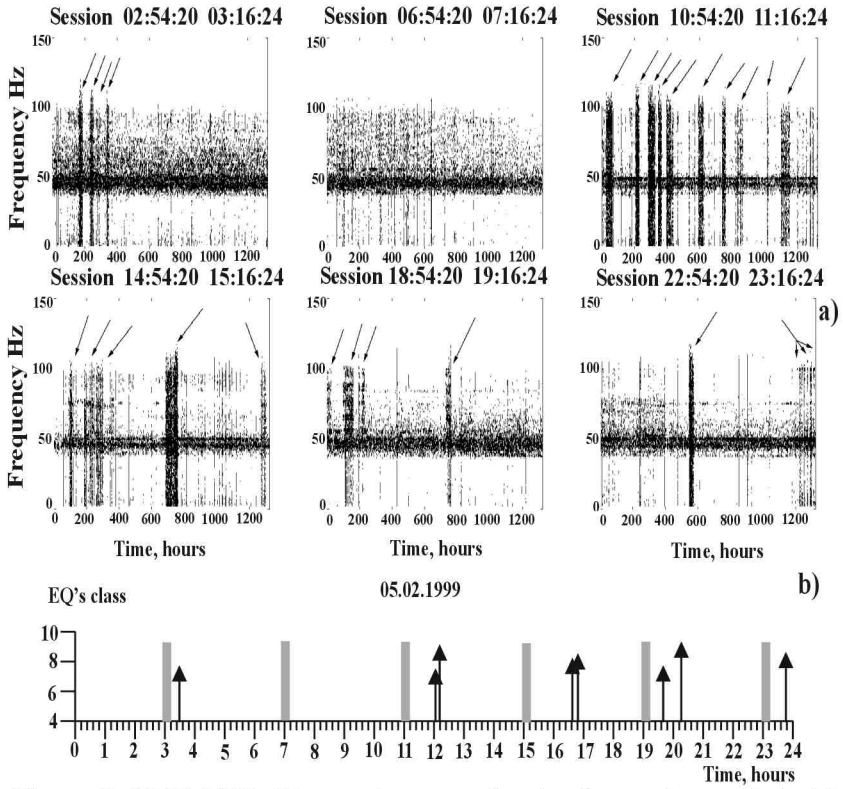

Figure 8. 05.02.1999. Six spectrograms for six observation periods (a) and the Regional Catalog fragment with the observation sessions made for the same day (b).

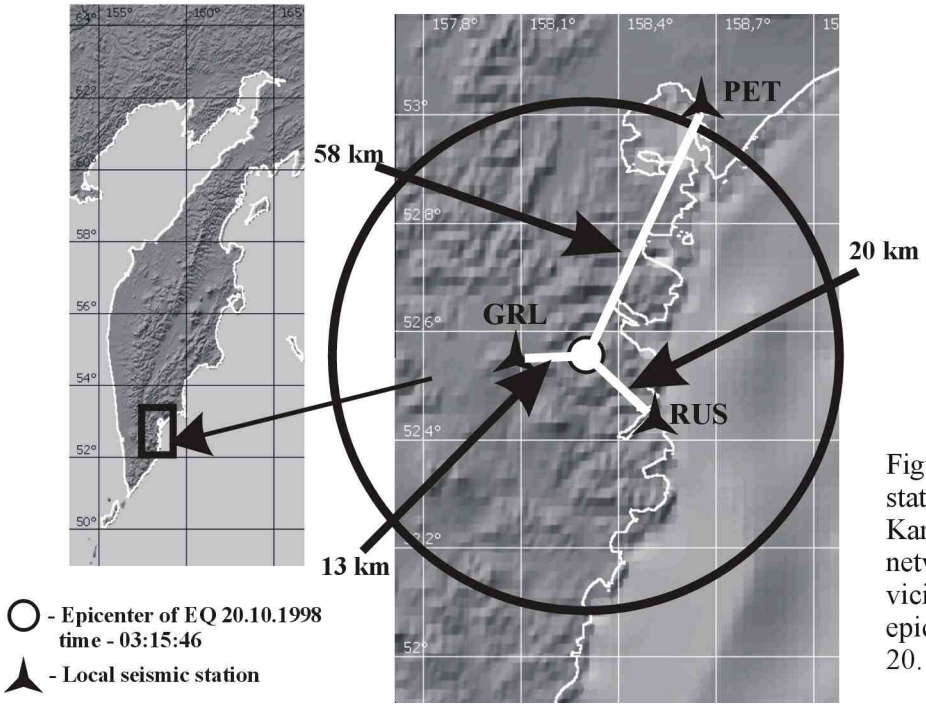

Figure 9. Three stations of the local Kamchatka seismic network located in the vicinity of the epicenter of the event 20.10.1998, 03:15:46.

Study of the hydroacoustic records allows detection of signals generated in the near-focus zone during the critical stage of the earthquake preparation. Surface seismographs are unable to detect them due to fast decay of the signal in solid rocks. The analysis of the HAS data enables us also to look closely into processes occurring in the epicentral zone during the stage preceding the major shock and to define the location of the source of the acoustic signals.

ACKNOWLEDGMENTS

The research was supported by the RFBR Grant No 01-05-64162 and by the Program of Leading Scientific Schools (Grant No 00-15-98583).

REFERENCES

Belyakov A. S., and Nikolaev A. V., 1995, Seismoacoustic observation methods. *The Physics of Earth*, 8, 89-93 (in Russian).

Beliakov A. S., Kuznetsov V. V., and Nikolaev A. V., 1991: Acoustical emission in the upper part of the Earth crust. *The Physics of Earth*, 10, 79-84 (in Russian).

Clay C.S., and Medwin H., 1977: *Acoustical Oceanography*, New York, J. Wiley, 576 p.

Demianovich V. V., 1998: How "Agam" was created. In: From the History of Russian Acoustics, Sankt-Petersburg, 295-315 (in Russian).

Karlik Ya. S., 2002: Hydroacoustic antenna: A powerful tool to forecast tsunamigenic earthquakes. (*present volume*)

Levin B. W., and Sassorova E. V., 1999: Low-frequency seismic signals as regional signs of the earthquake preparation. *Volcanology and Seismology*, 4-5, 108-115 (in Russian).

Michihiro K., Hata K., Fujiwara T., Yoshioka H., and Tanimoto T., 1989: Study on estimating initial stress and predicting failure on rock masses by acoustic emission. In: *Rock Mechanics and Rock Physics at Great Depth*. Rotterdam, 1025-1032.

Morozov V. E., 2002: High-frequency hydro-acoustic signals (40-110 Hz), foregoing the earthquakes, on the Pacific shelf of the Kamchatka Peninsula (*Present volume*).

Mostrioukov A. O., Lykov V. I., Patonin A. V., Petrov V. A., and Sassorova E. V., 2002: Preceding acoustic emission in the experiments "STICK-SLIP" as an analog of low-frequency earthquake precursors. Earth Sciences. Physics and Mechanics of Earth Materials. Moscow, Vuzovskaya Kniga, 94-104 (in Russian).

Ponomarev A. V., Zavjalov A. D., Smirnov V. B., Lockner D. A., 1997: Physical modeling of the formation and evolution of seismically active fault zones. *Tectonophysics*, 277, 57-81.

Rykunov L. N., Khavriushkin O. B., and Tsyplakov V. V., 1978: Apparatus and methods for investigating weak seismic effects. Moscow, VINITI, Dep.VINITI 29.08.78, # 2919-78, 31 p. (in Russian).

Rykunov L. N., Khavriushkin O. B., and Tsyplakov V. V., 1979: Time variations of high-frequency seismic noise. *The Physics of Earth*, 11, 72-77 (in Russian).

Rykunov L. N., and Smirnov B. V., 1992: Microscale seismology. *Volcanology and Seismology*, 3. 3-15 (in Russian).

Saltykov V. A., 1995: Peculiar properties of high-frequency relation of the seismic noise with lunar and solar tides. Dokl. AS, 341, 3, 406-407 (in Russian).

Saltykov V. A., Sinitsyn V. I., and Tchebrov V. N., 1997: Tidal component. Variations of the high-frequency seismic noise as a result of modifications in the medium stressed state. *Volcanology and Seismology*, 4, 73-84 (in Russian).

Saltykov V. A., Sinitsyn V. I., and Tchebrov V. N., 1998: High-frequency seismic noise application to the forecast of strong Kamchatka earthquakes. Kronotskoe Earthquake at Kamchatka on December 5, 1997: Precursors, Peculiarities, and Consequences. Edited by Gordeev E. I., Ivanov B. V., and Vikulin A. I., Petropavlovsk-Kamchatsky, KGARF, 99-105 (in Russian).

Sassorova E. V., and Levin B. W., 2001: The low frequency seismic signal foregoing a main shock as a sign of the last stage of earthquake preparation or preliminary rupture. *Physics and Chemistry of the Earth,* Part C, 26, (10-12), 775-780.

Sassorova E. V., Levin B. W., and Mostrioukov A. O., 2001: The low frequency seismic signal foregoing a main shock as a preparation sign of the large ocean earthquake. International Workshop "Tsunami Risk Assessment Beyond 2000". Moscow, 136-142.

Sheriff R. E., and Geldart L. P., 1995: Exploration Seismology. 2nd edition, Cambridge Univ. Press, 592 p.

Smirnov V. B., Ponomarev A. V., and Zavjalov A. D., 1995a: Peculiar properties of formation and evolution of the acoustic regime structure in rock samples. *Dokl. AS*, 343, 6, 818-823p. (in Russian).

Smirnov V. B., Ponomarev A. V., and Zavjalov A. D., 1995b: Structure of acoustic regime in rock samples. *Earth Physics*, 1, 38-58 (in Russian).

Smirnov V. B., Ponomarev A. V., and Sergeeva S. M., 2001: On similarity and feedback in the experiments on rock destruction. *Earth Physics*, 1, 89-96 (in Russian).

Sobolev G. A., 1993: Essential Principles of the Earthquake Forecast. Moscow, Nauka, 314 p. (in Russian).

Soloviev S. L., Ferry M., Kuzin I. P., and Kovachev S. A., 1989a: Seismicity of the Earth crust in the south-eastern part of the Tyrrhenian Sea (results of joint bottom and surface seismic observations). *Dokl. AS*, 305, 6, 1339-1343 (in Russian).

Soloviev S. L., Kovachev S. A., Kuzin I. P., and Tassos S., 1989b: Seismicity of the Earth crust in the southern part of the Aegean Sea (results of bottom seismic observations). *Dokl. AS*, **305**, 6, 1085-1089 (in Russian).

Vinogradov S. D., 1989: Acoustic Method in the Investigations on Earthquake Physics. O. Yu. Schmidt IPE AS USSR, Moscow, 177 p. (in Russian).

Virovlyansky A.L., Artel'ny V.V., and Stromkov A.A., 2000: Acoustic data obtained by hydrophone array off Kamchatka. Proc. US-Russia Workshop on Experimental Underwater Acoustics. IAP RAS, Nizhny Novgorod, 33-46.